

# Decreased NOTCH1 Activation Correlates with Response to Ibrutinib in Chronic Lymphocytic Leukemia



Beatrice Del Papa<sup>1</sup>, Stefano Baldoni<sup>1,2</sup>, Erica Dorillo<sup>1</sup>, Filomena De Falco<sup>1</sup>, Chiara Rompietti<sup>1</sup>, Debora Cecchini<sup>1</sup>, Maria Grazia Cantelmi<sup>1</sup>, Daniele Sorcini<sup>1</sup>, Manuel Nogarotto<sup>1</sup>, Francesco Maria Adamo<sup>1</sup>, Federica Mezzasoma<sup>1</sup>, Estevão Carlos Silva Barcelos<sup>1,3</sup>, Elisa Albi<sup>1</sup>, Roberta Iacucci Ostini<sup>1</sup>, Ambra Di Tommaso<sup>2</sup>, Andrea Marra<sup>1</sup>, Guido Montanaro<sup>1,4</sup>, Maria Paola Martelli<sup>1</sup>, Franca Falzetti<sup>1</sup>, Mauro Di Ianni<sup>4,5</sup>, Emanuela Rosati<sup>6</sup>, and Paolo Sportoletti<sup>1</sup>

## Abstract

**Purpose:** Ibrutinib, a Bruton tyrosine kinase inhibitor (BTKi), has improved the outcomes of chronic lymphocytic leukemia (CLL), but primary resistance or relapse are issues of increasing significance. While the predominant mechanism of action of BTKi is the B-cell receptor (BCR) blockade, many off-target effects are unknown. We investigated potential interactions between BCR pathway and NOTCH1 activity in ibrutinib-treated CLL to identify new mechanisms of therapy resistance and markers to monitor disease response.

**Experimental Design:** NOTCH1 activations was evaluated either *in vitro* and *ex vivo* in CLL samples after ibrutinib treatment by Western blotting. Confocal proximity ligation assay (PLA) experiments and analyses of down-targets of NOTCH1 by qRT-PCR were used to investigate the cross-talk between BTK and NOTCH1.

**Results:** *In vitro* ibrutinib treatment of CLL significantly reduced activated NOTCH1/2 and induced dephosphory-

lation of eIF4E, a NOTCH target in CLL. BCR stimulation increased the expression of activated NOTCH1 that accumulated in the nucleus leading to HES1, DTX1, and c-MYC transcription. Results of *in situ* PLA experiments revealed the presence of NOTCH1-ICD/BTK complexes, whose number was reduced after ibrutinib treatment. In ibrutinib-treated CLL patients, leukemic cells showed NOTCH1 activity downregulation that deepened over time. The NOTCH1 signaling was restored at relapse and remained activated in ibrutinib-resistant CLL cells.

**Conclusions:** We demonstrated a strong clinical activity of ibrutinib in a real-life context. The ibrutinib clinical efficacy was associated with NOTCH1 activity downregulation that deepened over time. Our data point to NOTCH1 as a new molecular partner in BCR signaling with potential to further improve CLL-targeted treatments.

<sup>1</sup>Institute of Hematology-Centro di Ricerca Emato-Oncologica (CREO), University of Perugia, Perugia, Italy. <sup>2</sup>Department of Life, Health and Environmental Sciences, Hematology Section, University of L'Aquila, L'Aquila, Italy. <sup>3</sup>Department of Biological Sciences, Postgraduate Program in Biotechnology (UFES), Federal University of Espirito Santo, Vitória-ES, Brazil. <sup>4</sup>Department of Hematology, Transfusion Medicine and Biotechnologies, Ospedale Civile, Pescara, Italy. <sup>5</sup>Department of Medicine and Aging Sciences, University of Chieti Pescara, Chieti, Italy. <sup>6</sup>Department of Experimental Medicine, Biosciences and Medical Embriology Section, University of Perugia, Perugia, Italy.

**Note:** Supplementary data for this article are available at Clinical Cancer Research Online (<http://clincancerres.aacrjournals.org/>).

B. Del Papa and S. Baldoni contributed equally to this article.

**Corresponding Author:** Paolo Sportoletti, University of Perugia, Piazzale Severi, Perugia 06132, Italy. Phone: 0039-075-578-2447; Fax: 0039-075-578-4109; E-mail: paolo.sportoletti@unipg.it

Clin Cancer Res 2019;25:7540-53

doi: 10.1158/1078-0432.CCR-19-1009

©2019 American Association for Cancer Research.

## Introduction

Recent years have shown a rapid expansion in our knowledge on the pathogenesis of chronic lymphocytic leukemia (CLL; ref. 1). This field of research has provided essential information for the development of innovative chemotherapy-free treatments.

Aberrant B-cell receptor (BCR) signaling is one of the mechanisms controlling survival of CLL cells (2). The Bruton tyrosine kinase (BTK), a key proximal kinase in the BCR pathway, is constitutively activated in CLL representing an ideal therapeutic target (3). Small-molecule inhibition of BTK represents a revolution in CLL management. Ibrutinib is the first-in-class drug for CLL treatment that irreversibly binds to the BTK activation site determining the inhibition of this enzyme (4). BTK inhibition reduced proliferation, survival, and migration of CLL cells to their growth-promoting microenvironment. Ibrutinib has been used as monotherapy for first-line and relapsed/refractory (R/R) CLL, with high response rates and prolonged progression-free (PFS) and overall survival (OS; ref. 5). Despite ibrutinib's activity in CLL, molecular effects other than BTK blocking are currently under investigation and drug resistance remains a challenge.

### Translational Relevance

B-cell receptor (BCR) signaling plays an integral role in B-cell malignancies' development, representing a suitable target for innovative therapy in chronic lymphocytic leukemia (CLL). Thus, the identification of molecular mechanisms underlying BCR inhibition and novel interaction partners of the BCR has the potential to further improve CLL-targeted treatments. We suggest that active Bruton tyrosine kinase (BTK) interacts with NOTCH1-ICD to maintain its levels, and that ibrutinib leads to NOTCH1-intracellular domain (ICD) downregulation by causing weakening of NOTCH1-ICD/BTK interactions. We demonstrated that the therapeutic response to ibrutinib is associated with the decrease of NOTCH1 activation, an important pathway for CLL pathogenesis. Our data point to the assessment of NOTCH1-ICD levels as a new marker of disease response and indicate NOTCH1 activation as an alternative mechanism underlying acquired resistance, independent of *BTK/PLCG2* mutations. It could therefore be advantageous to monitor NOTCH1 activation status in CLL under ibrutinib treatment for early detection of resistant clones and eventually inform further treatment choices. All these findings not only provide further support to ibrutinib therapy optimization, but also for its exploration in combination with anti-NOTCH1 agents in the setting of primary or acquired resistance.

Although the majority of ibrutinib-resistant CLL harbors *BTK* or *PLCG2* mutations (6), the identification of new molecular mechanisms of drug resistance will further improve CLL target treatment.

There is growing evidence that links CLL to activated NOTCH signaling (7, 8). CLL cells have a constitutive NOTCH1 and NOTCH2 activation contributing to apoptosis resistance (9). This finding led to the discovery of *NOTCH1* mutations in a fraction of patients with CLL with poor clinical outcome (10–14). Next-generation sequencing demonstrated that *NOTCH1* is one of the most frequently altered gene in the mutational landscape of CLL (15–17). *NOTCH1* mutations have a stabilizing effect on the NOTCH1 signaling of CLL cells that explains the constitutive pathway activation in 10%–20% mutated patients (18–21). More recently, it has been described a mechanism of NOTCH1 activation independent of the mutational status, based on the higher frequency of signaling activity compared with the incidence of the genetic lesion (22, 23). Altogether these findings indicated that NOTCH1 represents a key target in current and future CLL-tailored therapy.

To date, a functional interplay between the BCR and NOTCH1 signaling in CLL setting has never been investigated. Here, we discovered a novel inhibitory effect of ibrutinib against NOTCH1 activity *in vitro* and *in vivo*. We assessed the interaction between BCR stimulation and NOTCH1 pathway in primary CLL cells. In addition, we correlated the anti-NOTCH1 effects of ibrutinib to drug efficacy using the evaluation of NOTCH1 activity as a marker of disease monitoring and evolution. Our data will have the potential to further improve CLL treatments and to implement the use of current targeted agents against the BCR-associated BTK in CLL.

### Materials and Methods

#### Patients

Peripheral blood (PB) samples from patients with CLL were obtained after informed consent in accordance with the Declaration of Helsinki and under the approval of the specific local ethics committee (approval 2015–001 of the University of Perugia, Perugia, Italy). Clinical and biological characteristics are summarized in Supplementary Table S1.

#### CLL cells' isolation, culture, and stimulation

Neoplastic B cells were obtained from the blood of patients with CLL using Ficoll density-gradient centrifugation followed by sheep erythrocyte rosetting. This procedure allowed the separation of highly purified nonrosetting B leukemic cells from rosetting T cells. The average purity of CD19<sup>+</sup>/CD5<sup>+</sup> cells was 93.8% ± 2.7% as determined by flow cytometry (EPICS-XLMCL; Beckman Coulter) analysis using anti-CD45, CD19, CD5, CD11b, CD3 mAbs on 7AAD negative (all from Beckman Coulter). Cells were used fresh or viably frozen. Purified B cells were plated at 2 × 10<sup>6</sup>/mL in RPMI1640 media supplemented with 10% heat-inactivated human serum (FBS, Gibco-BRL), 2 mmol/L L-glutamine, and 100 U/mL penicillin/100 µg/mL streptomycin and were cultured in the presence or absence of DMSO (vehicle control), ibrutinib 1 or 10 µmol/L (ref. 24; PCI-32765 Selleckchem), and bepridil 2.5 µmol/L (ref. 25; Sigma-Aldrich) for 24 hours at 37°C in an atmosphere of 5% CO<sub>2</sub>. For experiments examining survival signals including stromal cocultures, HS-5 stromal cells (ATCC CRL-11882) were seeded at a concentration of 60,000 cells (80%–100% confluent) per well in 24-well plates, were incubated for 24 hours to allow cells to adhere, and 10<sup>6</sup> CLL cells were then added to the confluent layers of stromal cells in complete RPMI medium for 24 hours. For BCR stimulation experiments, isolated B-CLL cells from IGHV-unmutated patients were stimulated for 15 minutes with 10 µg/mL soluble AffiniPure F(ab')<sub>2</sub> Fragment Goat Anti-Human IgG+IgM (H+L) (Jackson ImmunoResearch Laboratories) and collected for the analysis of BTK phosphorylation and cleaved NOTCH1-ICD at the protein level. The transcriptional activity of NOTCH1-ICD was determined after 6-hour stimulation measuring the mRNA levels of NOTCH1 target genes.

#### Flow cytometry

Cell viability/apoptosis were assessed by flow cytometry after Annexin V-FITC/propidium iodide staining (Immunotech, Beckman Coulter). Results were expressed as the percentage of viable [Annexin V (AnV)–/propidium iodide (PI)–] or late apoptotic (AnV+/PI+) over vehicle-treated control. The analysis of NOTCH1 surface expression was performed using an anti-human NOTCH1-PE antibody (clone 527425, R&D Systems) or isotype control (mouse IgG1) gating on CD45<sup>+</sup>/CD19<sup>+</sup>/CD5<sup>+</sup> cells.

#### siRNA transfection

Transfection experiments were performed both in primary samples and in the PGA-1 (ACC 766) CLL cell line obtained from the German Collection of Microorganisms and Cell Cultures (DSMZ). Cells were transfected using the Amaxa Nucleofection Technology (Amaxa) and the ON-TARGETplus SMARTpool small-interfering RNA (siRNA) to total BTK (siBTK) or ON-

TARGETplus siCONTROL nontargeting pool (siCtrl) as negative control (Dharmacon RNA Technologies). CLL cells ( $12 \times 10^6$ ) were resuspended in 100  $\mu$ L Cell Line Solution Kit V (Lonza Group Ltd) with 0.25  $\mu$ mol/L of siBTK or siCtrl, transferred to the provided cuvettes and transfected with the Amaxa Nucleofector II device (program U-013). Cells were immediately transferred into 12-well plates in complete medium, and after 72 hours were examined for the expression of NOTCH1-ICD and BTK protein to verify the efficiency of silencing.

#### Western blotting

Whole-cell lysates were extracted as reported previously (9). Subcellular fractionation was performed using a NE-PER Nuclear and Cytoplasmic Extraction Reagent (Thermo Fisher Scientific), according to manufacturer's instructions. Western blotting was performed using the primary antibodies detailed in Supplementary Table S2. Densitometric analysis was done using Quantity One software.

#### Confocal immunofluorescence microscopy

Cells ( $2 \times 10^5$ ) were seeded on poly-L-lysine-coated micro coverglasses and fixed with 4% paraformaldehyde for 15 minutes at room temperature. Cells were then permeabilized with Triton X-100 (0.1% in PBS for 5 minutes at room temperature. After three washes in PBS with Triton X-100 (0.01%), cells were blocked with blocking buffer (1% BSA in PBS) for 30 minutes before 1-hour incubation at room temperature with rabbit anti-NOTCH1 (Val1744) and mouse anti-BTK antibodies (Supplementary Table S2) diluted in blocking buffer. After three washes in PBS with Triton X-100 (0.01%), cells were incubated with goat anti-rabbit Alexa Fluor 488 and goat anti-mouse Alexa-Fluor 568 for 40 minutes in the dark. Nuclei were stained with 4,6-Diamidino-2-phenyl indole (DAPI) in ProLong Gold antifade mounting reagent (Thermo Fisher Scientific). Images were acquired with a laser scanning confocal microscope LSM 800 with Airyscan (Zeiss) using a 63 $\times$  oil immersion and 1.4 NA objective (scale bar, 10  $\mu$ m).

#### Proximity ligation assay

The *in situ* proximity ligation assay (PLA) was applied to examine the interaction between NOTCH1-intracellular domain (ICD) and BTK in patients with CLL with positive ICD of NOTCH1, referred to as ICN1+. PLA was performed on fixed primary CLL cells with DuoLink PLA technology probes and reagents (Sigma-Aldrich), and following the manufacturer's protocol. Briefly, B cells from patients with CLL were permeabilized in 0.1% Triton X-100 in PBS, then blocked in 1% BSA, 0.01% Triton X-100 in PBS, and incubated with rabbit anti-NOTCH1 (Val1744) and mouse anti-BTK antibodies (Supplementary Table S2). Incubation with Duolink MINUS and PLUS probes conjugated to secondary antibody, ligation, and amplification steps for PLA were performed as suggested by the manufacturer using 40- $\mu$ L volume reaction. Following amplification, slides were washed for 10 minutes in Buffer A and B, and mounted with Duolink In Situ Mounting Medium containing DAPI. Negative controls were obtained by omitting primary antibodies. Fluorescent images were obtained using a confocal microscope LSM 800 (Zeiss) with Airyscan using a 63 $\times$  oil immersion and 1.4 NA objective (scale bar, 10  $\mu$ m). Ten fields were analyzed.

#### Real-time qPCR

RNA was extracted using RNeasy Plus Kits (Qiagen) and cDNA was obtained using Prime Script RT Master Mix (Takara Bio). We used the PCR Master Mix Power SYBER Green and the 7900HT fast Real-Time PCR System (Applied Biosystems). The primer sequences are included in Supplementary Table S3. Relative fold change was normalized to GAPDH and calculated using the  $2^{-\Delta/\Delta C_t}$  method.

#### Droplet digital PCR

NOTCH1 probe assays (dHsaCP2500500 and dHsaCP2500501, Bio-Rad) were used to determinate the allelic burden of NOTCH1. The droplet generated included DNA, NOTCH1 probes assays (1 $\times$ ), and ddPCR Supermix (2 $\times$ ) for Probes (no dUTP; Bio-Rad). The mix was amplified by PCR and analyzed by QX200 Droplet Reader (Bio-Rad). Scatterplots depict droplet digital PCR (ddPCR) results specifically for the NOTCH1 mutation assay.

#### Genetic analysis

Genomic DNA was extracted with the QIAamp DNA Blood Mini Kit (Qiagen). Genetic alterations analysis was performed accordingly to previously published protocols (25–27).

Specifically, the NOTCH1 mutation screening was performed using an allele-specific PCR method with two external primers as internal PCR control and a third primer specific for the mutation (25). BTK and PLCG2 mutations were detected by Sanger sequencing methods using primer sequences included in Supplementary Table S3. IGHV mutational status was analyzed according to ERIC recommendations (28).

#### Statistical analysis

Statistical analyses were performed with GraphPad Software. Statistical differences between mean values were evaluated using nonparametric tests as Wilcoxon for paired data and Mann–Whitney for nonpaired data. One-way ANOVA with Tukey *post hoc* test was performed to test significant differences between multiple groups. Survival was calculated from the start of ibrutinib to the date of progression (PFS) or death (OS) using the Kaplan–Meier method.

## Results

### BCR inhibition by ibrutinib impairs NOTCH signaling in CLL cells *in vitro*

To investigate whether BTK suppression affected the NOTCH1 pathway *in vitro*, we treated for 24 hours with ibrutinib 10  $\mu$ mol/L primary CLL cells exhibiting activated intracellular form of NOTCH1, referred to as ICN1+ CLL ( $N = 14$ ). NOTCH1 activation levels were measured by Western blotting using the anti-NOTCH1 (Val1744) antibody, which recognizes the cleaved NOTCH1 ICD starting at Val1744. Notably, ibrutinib-treated CLL showed a significant lower expression of NOTCH1-ICD compared with cells cultured with vehicle ( $P < 0.001$ ; Fig. 1A, left and middle). Our data demonstrated a significant NOTCH1-ICD reduction in both NOTCH1-mutated ( $N = 6$ ;  $P < 0.05$ ) and NOTCH1 wild-type samples ( $N = 8$ ;  $P < 0.01$ ; Fig. 1A, right) treated with ibrutinib compared with vehicle.

We further confirmed this inhibitory effect using an antibody against all forms of NOTCH1 ( $N = 17$ ) that showed significant NOTCH1-ICD downregulation ( $P < 0.001$ ) associated with lower

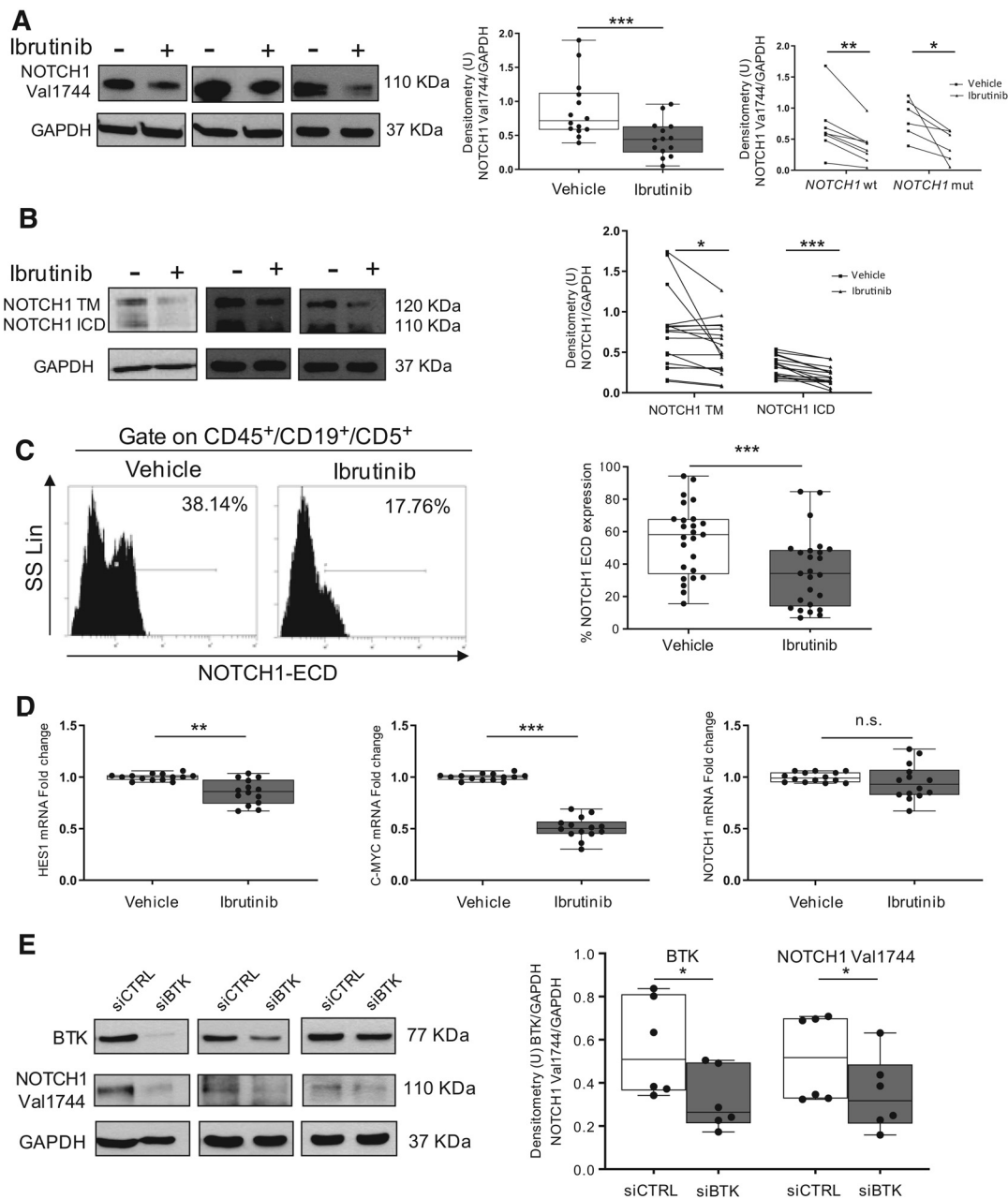


**Figure 1.**

The antitumor efficacy of ibrutinib was associated with inhibition of NOTCH1 activity *in vitro*. **A**, The representative blots of the activated NOTCH1-ICD [NOTCH1 (Val1744)] protein levels in CLL cells treated with ibrutinib (10  $\mu$ mol/L) for 24 hours compared with vehicle controls (DMSO). The box-and-whisker plot with data points in the middle panel shows densitometric Western blot data in the total cohort of patients with CLL ( $N = 14$ , left). Dot and line diagram of the densitometric Western blot data analyzed in the context of *NOTCH1* wild-type (wt;  $N = 8$ ) and *NOTCH1*-mutated (mut;  $N = 6$ ) patients with CLL. Densitometry units (U) were calculated relative to GAPDH (right). **B**, The representative blots using an antibody against the TM and ICD forms of NOTCH1 protein in CLL cells treated with ibrutinib (10  $\mu$ mol/L) for 24 hours compared with vehicle controls (DMSO, left). Dot and line diagram of the densitometric Western blot data of 17 patients. Densitometry units (U) were calculated relative to GAPDH (right). **C**, Representative flow cytometry histogram of the percentage of the extracellular domain (ECD) of NOTCH1 in CD45<sup>+</sup>/CD19<sup>+</sup>/CD5<sup>+</sup> CLL cells incubated for 24 hours with ibrutinib (10  $\mu$ mol/L) or vehicle control (DMSO, left). The box-and-whisker plot with data points in the right panel shows NOTCH1-ECD fluorescence in 25 patients. **D**, Box-and-whisker plots with data points show the analysis of HES1 (left), c-MYC (middle), and NOTCH1 (right) mRNA in CLL cells treated with ibrutinib (10  $\mu$ mol/L) for 6 hours ( $N = 14$ ). mRNA levels were normalized to GAPDH and represented as fold change using vehicle control (DMSO) cells as a reference. \*\*\*,  $P < 0.001$ ; \*\*,  $P < 0.01$ ; \*,  $P < 0.05$ ; and n.s., not significant (ibrutinib vs. vehicle) according to Wilcoxon paired test. **E**, The representative blots of total BTK and activated NOTCH1-ICD [NOTCH1(Val1744)] protein levels in the PGA-1 CLL cell line (left blot) and two primary samples (middle and right blots) transfected with control siRNA (siCtrl) or BTK siRNA (siBTK; left). The box-and-whisker plot with data points in the right shows densitometric Western blot data of six independent experiments. Densitometry units (U) were calculated relative to GAPDH. \*,  $P < 0.05$  (siBTK vs. siCtrl) according to Wilcoxon paired test.

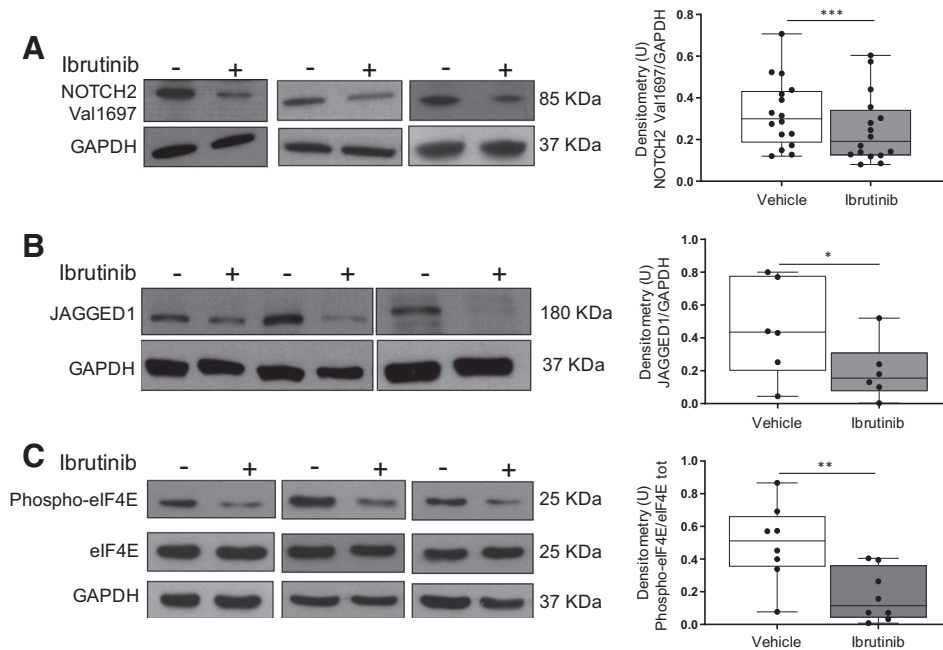
transmembrane (TM) domain levels ( $P < 0.05$ ; Fig. 1B). In addition, flow cytometry demonstrated that also the percentage of the extracellular domain (ECD) of NOTCH1 ( $N = 25$ ) was significantly reduced in ibrutinib-treated CLL compared with vehicle ( $P < 0.001$ ; Fig. 1C). The impaired NOTCH1 activity was associated with a significant reduction of HES1 ( $P < 0.01$ ) and c-MYC ( $P < 0.001$ ) mRNA levels ( $N = 14$ ; Fig. 1D, left and middle), well-known downstream targets of the NOTCH1 signaling pathway. Conversely, NOTCH1 mRNA expression was similar in CLL cells treated with ibrutinib and vehicle ( $N = 14$ ; Fig. 1D, right), suggesting that NOTCH1 transcription was not affected. The inhibitory effects of ibrutinib on the levels of different subunits of the NOTCH1 protein and on the mRNA expression of its target genes were independent of the IGHV mutational status of CLL cells, being similar in both IGHV-mutated and unmutated samples (Supplementary Fig. S1A–S1D). Given the key role of microenvironmental signals in increasing NOTCH1 signaling, we tested the anti-NOTCH1 activity of ibrutinib in CLL cultured on a stromal layer ( $N = 6$ ). As shown in Supplementary Fig. S2, the effects of BTK inhibition preserved the capacity to switch-off NOTCH1 under coculture conditions ( $P < 0.05$ ).

To exclude potential nonspecific effects of ibrutinib, we downregulated the expression of total BTK protein in the PGA-1 CLL cell line and primary samples using siRNA. CLL cells were treated with BTK siRNA (siBTK), cultured for 48 hours

in complete medium, and then analyzed for total BTK and NOTCH1-ICD expression ( $N = 6$ ). As shown in Fig. 1E, the reduction of BTK expression induced by siBTK was accompanied by decreased levels of NOTCH1-ICD suggesting a crosstalk between BTK and NOTCH1 signaling. In keeping with these results, we demonstrated that ibrutinib maintained the ability to significantly reduce ( $P < 0.05$ ) NOTCH1-ICD ( $N = 7$  and  $N = 6$ ; Supplementary Fig. S3A and S3B, respectively), NOTCH1-TM ( $N = 6$ ; Supplementary Fig. S3B) and NOTCH1-ECD ( $N = 10$ ; Supplementary Fig. S3C) even when used at  $1 \mu\text{mol/L}$ , the concentration required to inhibit BTK activity in CLL cells *in vitro*.

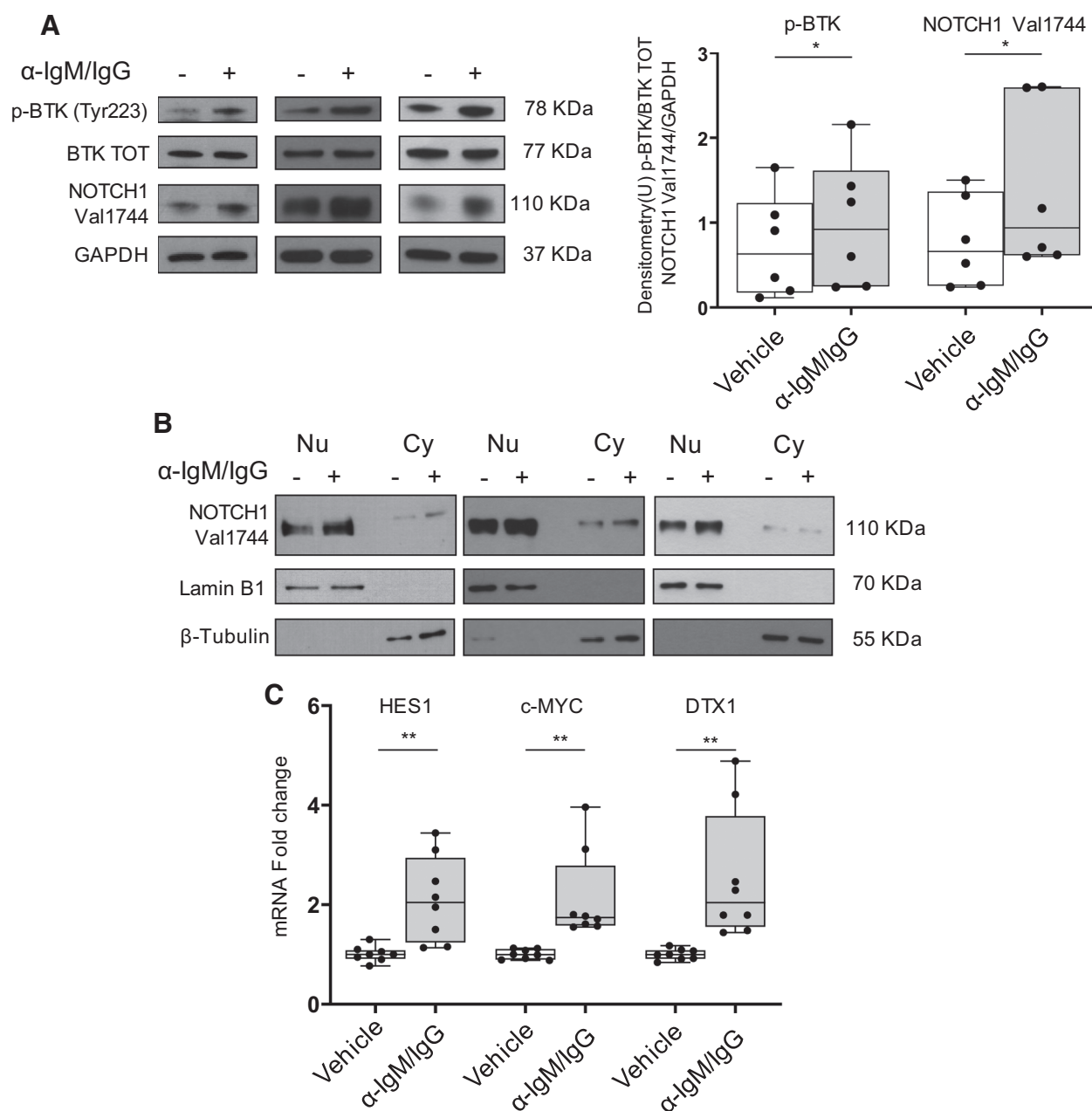
Besides NOTCH1 activation, CLL constitutively overexpressed active NOTCH2 along with higher levels of JAGGED1 ligand compared with normal B cells (9, 29). We demonstrated that ibrutinib efficiently reduced the levels of both activated NOTCH2 ( $N = 16$ ;  $P < 0.001$ ) and JAGGED1 ( $N = 6$ ;  $P < 0.05$ ) expression in CLL, compared with vehicle after 24-hour treatment (Fig. 2A and B).

We recently demonstrated that NOTCH1/2 targeting is accompanied by reduced phosphorylation of eukaryotic translation initiation factor 4E (eIF4E; ref. 30), suggesting that this protein is another NOTCH target in CLL. To further demonstrate the anti-NOTCH activity of ibrutinib, we examined its effect on eIF4E phosphorylation ( $N = 8$ ). As shown in Fig. 2C, ibrutinib treatment reduced the levels of



**Figure 2.**

Effects of ibrutinib on NOTCH2 activity, JAGGED1 expression and eIF4E phosphorylation. **A**, Representative blots (left) and quantitative densitometry analysis (right; box-and-whisker plot with data points,  $N = 16$ ) of the activated ICD of NOTCH2 [NOTCH2(Val1697)] protein levels in CLL cells treated with ibrutinib ( $10 \mu\text{mol/L}$ ) for 24 hours compared with vehicle controls. Densitometry units (U) were calculated relative to GAPDH. **B**, Representative blot (left) and quantitative densitometry analysis (right; box-and-whisker plot with data points,  $N = 6$ ) of JAGGED1 protein levels in CLL cells treated with ibrutinib ( $10 \mu\text{mol/L}$ ) for 24 hours compared with vehicle controls. Densitometry units (U) were calculated relative to GAPDH. **C**, Representative blots (left) and quantitative densitometry analysis (right; box-and-whisker plot with data points,  $N = 8$ ) of total and phosphorylated forms of eIF4E protein levels in CLL cells treated with ibrutinib ( $10 \mu\text{mol/L}$ ) for 24 hours compared with vehicle controls. Densitometry units (U) were calculated relative to total eIF4E. \*\*\*,  $P < 0.001$ ; \*\*,  $P < 0.01$ ; and \*,  $P < 0.05$  (ibrutinib vs. vehicle) according to Wilcoxon paired test.

**Figure 3.**

BCR stimulation enhances NOTCH1 signaling activation in CLL cells. **A**, The representative blots of phosphorylated BTK (p-BTK), total BTK, and activated NOTCH1-ICD [NOTCH1(Val1744)] performed on whole-cell lysates of IgM/IgG stimulated and unstimulated CLL cells ( $N = 6$ ). Protein loading was assessed using an anti-GAPDH antibody (left). A box-and-whisker plot with data points ( $N = 6$ ) of densitometry analysis of the Western blot staining for p-BTK and NOTCH1-ICD that were calculated relative to total BTK and GAPDH, respectively (right). **B**, Representative Western blot analysis of NOTCH1-ICD [NOTCH1 (Val1744)] performed in nuclear (Nu) and cytoplasmic (Cy) extracts from CLL cells after IgM/IgG stimulation for 15 minutes. Adequate fractionation and protein loading were assessed using anti-lamin B1 and anti- $\beta$ -tubulin antibodies. Data shown are representative of six patients examined. **C**, The box-and-whisker plot with data points shows analysis of *HES1*, *c-MYC*, and *DTX1* gene expression in CLL cells after IgM/IgG stimulation for 6 hours ( $N = 8$ ). mRNA levels were normalized to GAPDH and represented as fold change using unstimulated cells as a reference. \*\*,  $P < 0.01$ ; \*,  $P < 0.05$  (stimulus vs. vehicle) according to Wilcoxon paired test.

phosphorylated-eIF4E ( $P < 0.01$ ) but not of its expression compared with untreated cells. These data reveal that ibrutinib displays an anti-NOTCH effect in CLL that impacts the levels

and transcriptional activity of NOTCH1/2 and the expression of JAGGED1, implying a potential interplay between the BCR and NOTCH pathways.

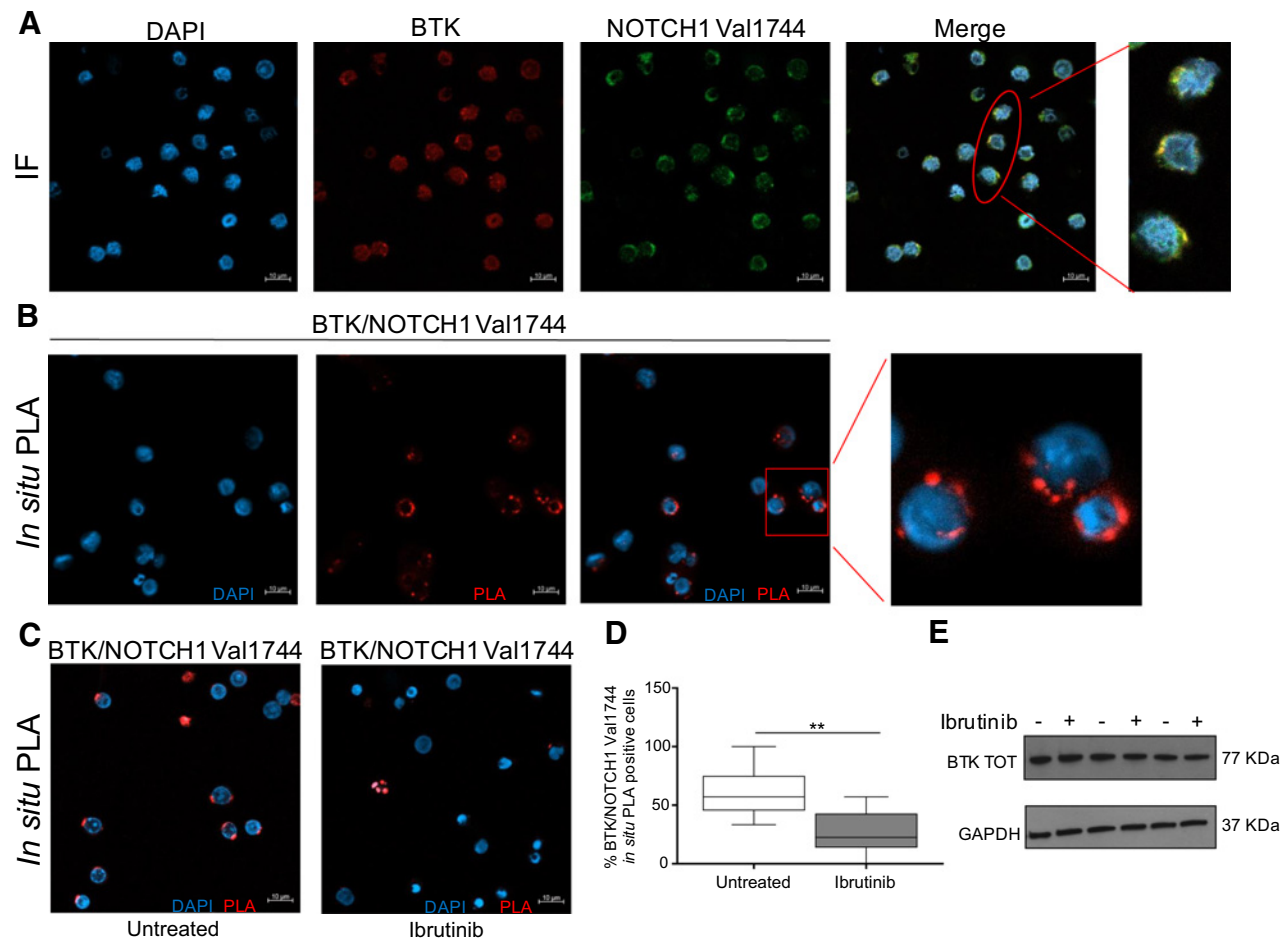


**Figure 4.**

Colocalization and physical interactions of BTK and NOTCH1-ICD in CLL cells. **A**, Representative confocal images showing cytoplasmic colocalization of BTK and NOTCH1-ICD. CLL cells were stained with mouse anti-BTK (red) and rabbit anti-NOTCH1-ICD [NOTCH1(Val1744)] (green) antibodies. Nuclei were stained with DAPI (blue). Merged panel depicts the merge three-color confocal image showing colocalization of BTK and NOTCH1-ICD in DAPI-stained cells. Images were acquired on a confocal microscope LSM 800 (Zeiss) with Airyscan using a 63× oil immersion and 1.4 NA objective (scale bar, 10 μm). Data shown are representative of three patients. **B**, Representative images of *in situ* PLA showing the interaction between BTK and NOTCH1-ICD under basal conditions. *In situ* PLA was performed using mouse anti-BTK and rabbit anti-NOTCH1-ICD [NOTCH1(Val1744)] antibodies (see Materials and Methods section for details). Nuclei were stained with DAPI. Red spots indicate PLA-positive cells. Images were acquired using confocal microscopy using a 63× oil immersion and 1.4 NA objective (scale bar, 10 μm). **C–D**, Ibrutinib treatment for 24 hours induces a significant decrease of PLA-positive cells, indicating that BTK inhibition leads to destabilization of BTK/NOTCH1-ICD complexes. Box-and-whisker plot showing quantitative analysis of the PLA signals of 10 fields per sample. \*\*,  $P < 0.01$  according to Wilcoxon paired test. **E**, Representative blots of total BTK protein in CLL cells treated for 24 hours with ibrutinib (10 μmol/L) compared with untreated controls ( $N = 3$ ).

**BCR stimulation increases NOTCH1 signaling pathway in CLL cells *in vitro***

To further investigate the cross-talk between BCR and NOTCH1 signaling, we determined whether BCR engagement influenced NOTCH1 activation. We incubated CLL cells from IGHV-unmutated samples for 15 minutes with soluble anti-IgM/IgG antibodies known to activate the BCR ( $N = 6$ ). Results showed that BCR stimulation induced BTK phosphorylation ( $P < 0.05$ ), indicating an effective responsiveness of CLL cells (Fig. 3A). Strikingly, the levels of NOTCH1-ICD were significantly upregulated ( $P < 0.05$ ) in BCR-stimulated cells compared with unstimulated controls (Fig. 3A).

To determine whether this induction of NOTCH1 increased its transcriptional activity, we examined NOTCH1-ICD nuclear translocation ( $N = 6$ ) and mRNA expression ( $N = 8$ ) of the NOTCH1

target genes *HES1*, *c-MYC*, and *DTX1* (31). Western blot analysis of nuclear and cytoplasmic fractions of unstimulated CLL showed that NOTCH1-ICD was almost completely localized in nuclear extracts (Fig. 3B), consistent with constitutive NOTCH1 activation. After BCR stimulation, the NOTCH1-ICD nuclear levels (Fig. 3B), as well as *HES1*, *c-MYC*, and *DTX1* expression (Fig. 3C) increased  $2.15 \pm 0.96$ -fold,  $2.13 \pm 0.86$ -fold, and  $2.56 \pm 1.3$ -fold, respectively, compared with unstimulated controls ( $P < 0.01$ ).

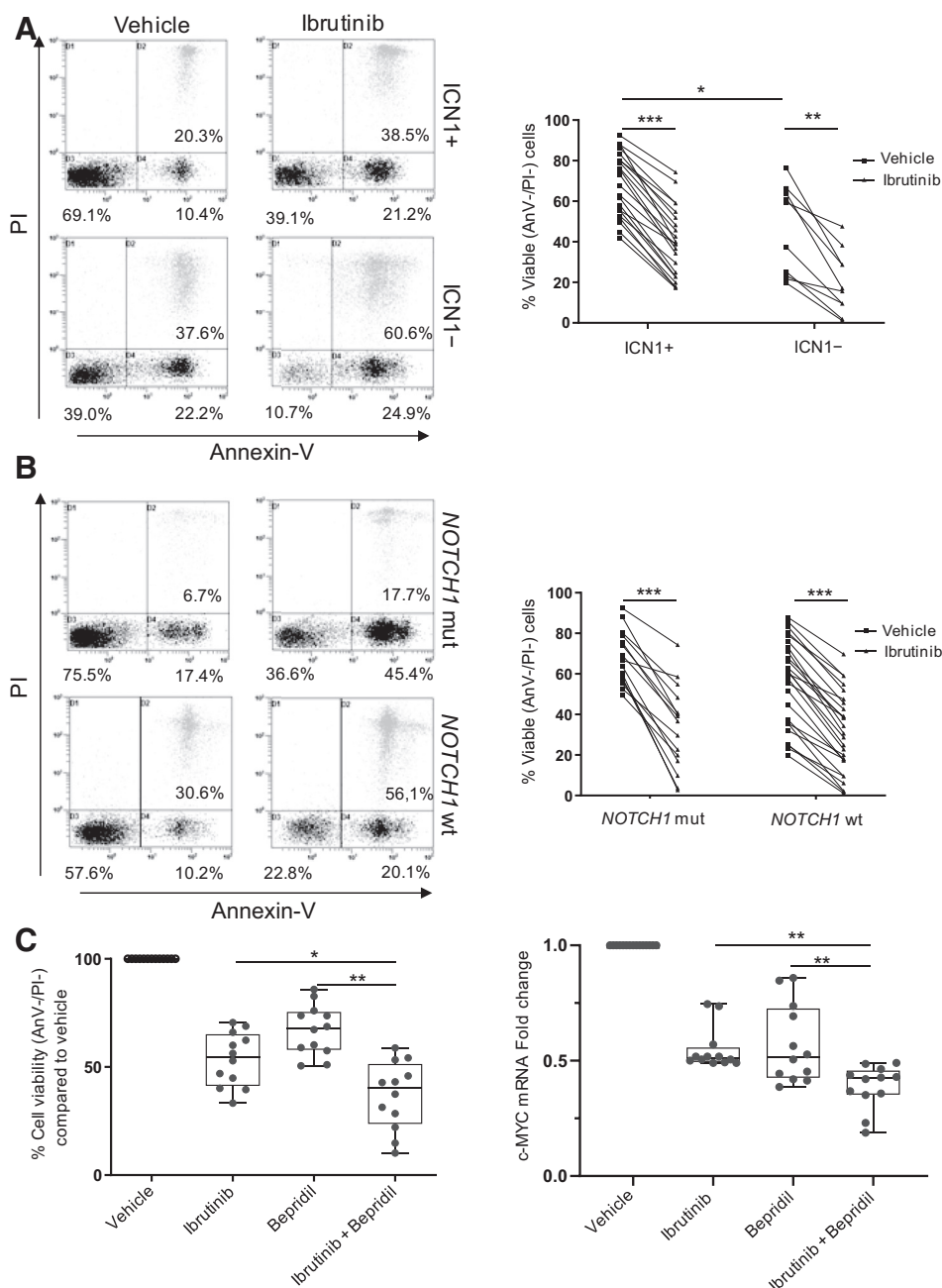
These data support the hypothesis of BTK as one of the potential kinases regulating NOTCH1 activation in CLL.

**BTK associates with NOTCH1-ICD in primary CLL cells**

We investigated the possibility that BTK interacts with the NOTCH1-ICD protein in primary CLL cells from ICN+ patients. First, we performed immunofluorescence using confocal

**Figure 5.**

The cytotoxic effects of ibrutinib depend on NOTCH1 and increase the anti-NOTCH1 activity of bepridil *in vitro*. **A**, Representative dot plots (left) and dot and line diagram (right) of Annexin V-FITC/PI staining results of viability in ibrutinib-treated CLL cells exhibiting or lacking the activated intracellular form of NOTCH1, indicated as ICN1+ ( $N = 22$ ) and ICN- ( $N = 10$ ), respectively. CLL cells were cultured in the presence of ibrutinib 10  $\mu\text{mol/L}$  or vehicle (DMSO) for 24 hours before Annexin V-FITC/PI staining. \*\*\*,  $P < 0.001$ ; \*\*,  $P < 0.01$ ; \*,  $P < 0.05$  according to Mann-Whitney for unpaired data and Wilcoxon for paired test. **B**, Representative dot plots (left) and dot and line diagram (right) of Annexin V-FITC/PI staining results of viability in ibrutinib-treated CLL cells with a mutated (*NOTCH1* mut;  $N = 15$ ) or wild-type (*NOTCH1* wt;  $N = 26$ ) *NOTCH1* gene. \*\*\*,  $P < 0.001$  according to Wilcoxon for paired test. **C**, Left, a box-and-whisker plot with data points of Annexin V-FITC/PI staining results of viability of ICN1+ CLL cells after 24-hour treatment with the combination of ibrutinib 10  $\mu\text{mol/L}$  and bepridil 2.5  $\mu\text{mol/L}$  compared to single treatment ( $N = 12$ ). Right, a box-and-whisker plot with data points of the analysis of c-MYC mRNA in ICN1+ CLL cells after 6-hour treatment with the combination of ibrutinib and bepridil ( $N = 12$ ). mRNA levels were normalized to GAPDH and represented as fold change using vehicle-treated cells as a reference. One-way ANOVA with Tukey *post hoc* test were performed to test for significant differences between multiple groups (\*,  $P < 0.05$ ; \*\*,  $P < 0.01$ ).



microscopy to define whether these two proteins reside at the same physical location in CLL cells ( $N = 3$ ). Our data demonstrated overlapping distribution of total BTK and NOTCH1-ICD proteins in the cytoplasm of leukemic cells (Fig. 4A). Furthermore, we investigated the BTK/NOTCH1-ICD interaction using *in situ* PLA ( $N = 3$ ), a highly sensitive technology extending the capabilities of traditional immunoassay to detect molecular interactions. Under basal conditions, CLL cells showed the presence of several red spots representing single protein-protein interaction with a cytoplasmic localization (Fig. 4B). *In vitro* treatment with 10  $\mu\text{mol/L}$  ibrutinib for 24 hours resulted in significant decrease in the percentage of CLL cells showing red spots (Fig. 4C and D). Nevertheless, Western blot analysis indicated that BTK total

protein was not degraded ( $N = 3$ ; Fig. 4E). Altogether, these data indicated that ibrutinib leads to destabilization of BTK/NOTCH1-ICD complexes in CLL without affecting BTK expression.

**Ibrutinib-induced CLL cytotoxicity *in vitro* is influenced by NOTCH1 activation status, but is independent of NOTCH1 mutation**

To determine the functional relevance of the anti-NOTCH activity of ibrutinib, we analyzed its cytotoxic effects on CLL in the context of NOTCH1 activation and mutation. First, we compared ICN1+ CLL ( $N = 22$ ) to cells lacking NOTCH1-ICD ( $N = 10$ ), referred to as ICN1 negative (ICN1-). In untreated cells, ICN1+ cell viability was higher than ICN1- ( $P < 0.05$ ).

Downloaded from <http://aacrjournals.org/clinccancerres/article-pdf/25/24/7540/2055978/7540.pdf> by guest on 21 May 2025



Ibrutinib 10  $\mu\text{mol/L}$  treatment significantly reduced viability and increased apoptosis of both ICN1+ ( $P < 0.001$ ) and ICN1- ( $P < 0.01$ ) CLL compared with controls (Fig. 5A). Remarkably, the percentage of reduction in cell viability induced by ibrutinib and normalized to the respective vehicle control, was higher in ICN1- than in ICN1+ cells ( $61.6\% \pm 22.3\%$  vs.  $44.5\% \pm 14.5\%$ ;  $P < 0.05$ ; Supplementary Fig. S4A), indicating that the lack of NOTCH1 activation renders cells more sensitive to the apoptotic effect of the drug. These data suggest that anti-NOTCH1 activity of ibrutinib represents an additional effect on cell death induction and lead us to hypothesize that NOTCH1 activation confers an increased CLL cell fitness against the antileukemic effects of BTKi.

It has been shown that NOTCH1-mutated CLL are associated with higher NOTCH1 activation and drug resistance compared

with NOTCH1 wild-type CLL (18). We measured the impact of NOTCH1 mutations on the cytotoxic effects of ibrutinib 10  $\mu\text{mol/L}$ . As previously shown, spontaneous apoptosis is higher in NOTCH1 wild-type compared with mutated (18, 19). Compared with vehicle, ibrutinib reduced cell viability and increased apoptosis to a similar extent in either NOTCH1-mutated ( $N = 15$ ) or wild-type ( $N = 26$ ) CLL (Fig. 5B; Supplementary Fig. S4B), suggesting that the cytotoxic effect depended on NOTCH1 activity regardless its genetic alteration. In keeping with this observation, no differences emerged even when comparing CLL with high versus low NOTCH1 mutational burden (Supplementary Fig. S5).

In line with previous reports, ibrutinib 1  $\mu\text{mol/L}$  was associated with a moderate reduction of CLL cell viability that was still significant in the context of samples with activated (ICN+;  $N =$

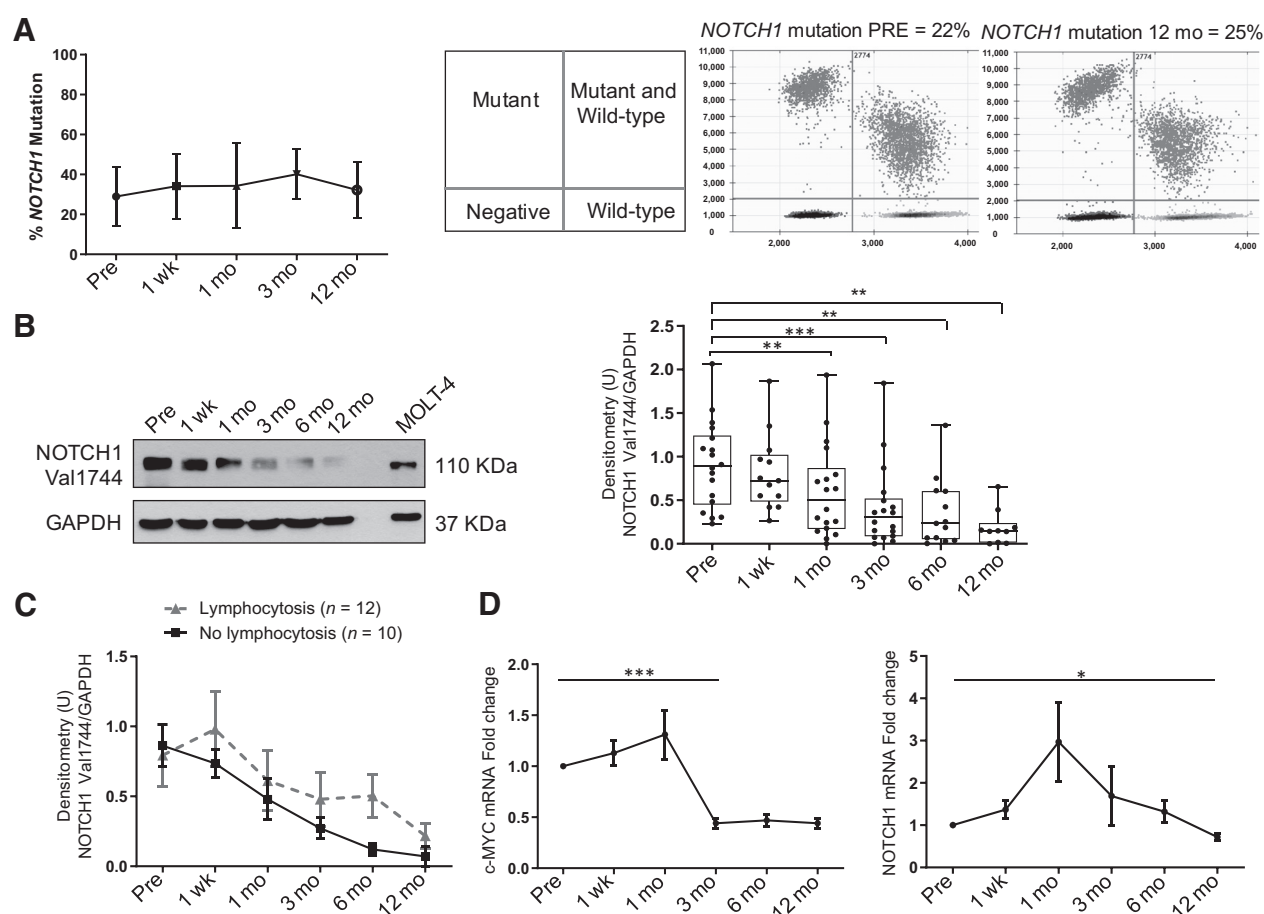


**Figure 6.** Ibrutinib downregulates NOTCH1 activity in serial samples from CLL-treated patients. **A**, Kinetics of the NOTCH1-mutated clone in three patients with CLL longitudinally investigated by ddPCR during ibrutinib treatment. A schematic representation of positive and negative droplet distribution according to the fluorophore threshold indicated in lines and representative scatterplots depicting ddPCR results specifically for the NOTCH1 mutation assay in one sample before (PRE) and 12 months (mo) after ibrutinib treatment. **B**, Representative Western blot analysis of the activated NOTCH1-ICD [NOTCH1(Val1744)] protein levels in serial samples of a ibrutinib-treated CLL patient within a 12-month period (left). The box-and-whisker plot with data points on the right represent a quantitative densitometry analysis of the Western blot staining for NOTCH1(Val1744) in the cohort of 18 ibrutinib-treated patients overtime. Densitometry units (U) were calculated relative to GAPDH. **C**, Kinetics of activated NOTCH1-ICD [NOTCH1(Val1744)] expression in ICN1+ CLL cases split according to ibrutinib-related lymphocytosis, shown as mean values. The number of patients included in each group are reported in parentheses; the error bars indicate SEM. **D**, Time course of NOTCH1 and c-MYC mRNA expression in CLL cells collected in 25 ibrutinib-treated patients at the indicated timepoints. mRNA levels were normalized to GAPDH and represented as fold change using the baseline (Pre) as a reference. Results are the mean  $\pm$  SEM. \*\*\*,  $P < 0.001$ ; \*\*,  $P < 0.01$ ; and \*,  $P < 0.05$  according to Wilcoxon paired test.

10;  $P < 0.01$ ), unactivated (ICN $^-$ ;  $N = 8$ ;  $P < 0.01$ ; Supplementary Fig. S6A), mutated ( $N = 7$ ;  $P < 0.05$ ), and wild-type *NOTCH1* ( $N = 11$ ;  $P < 0.01$ ; Supplementary Fig. S6B).

#### The combination of ibrutinib with the anti-NOTCH1 small-molecule bepridil enhances CLL cell death *in vitro*

The data above indicate the need for combination therapy that may be more effective against the NOTCH1 signaling to overcome the reduced efficacy of ibrutinib toward ICN1+ CLL. Recently, we identified bepridil (32) as an alternative approach to the  $\gamma$ -secretase inhibitor (GSI)-based NOTCH1 inhibition and a promising candidate for CLL target therapy. We used ibrutinib 10  $\mu\text{mol/L}$  in combination with bepridil to analyze their cytotoxic effects on ICN1+ CLL *in vitro* ( $N = 12$ ). After 24-hour treatment, flow cytometry showed a significant reduction of cell viability and a strong apoptotic induction by drug combination compared with single treatment normalized with vehicle control ( $P < 0.05$  and  $P < 0.01$ ; Fig. 5C, left). The antileukemic effect of ibrutinib and bepridil combination also correlated with a significant downregulation of the NOTCH1 target *c-MYC* measured after 6-hour treatment ( $N = 12$ ;  $P < 0.01$ ; Fig. 5C, right). Significant effects on cell viability ( $N = 14$ ;  $P < 0.05$  and  $P < 0.001$ ) and *c-MYC* mRNA expression ( $N = 14$ ;  $P < 0.01$  and  $P < 0.001$ ) were also observed when we compared the combination of ibrutinib 1  $\mu\text{mol/L}$  and bepridil (Supplementary Fig. S6C). Altogether, these data indicate that the NOTCH1 inhibitor bepridil enhances the antileukemic activity of ibrutinib and its ability to downregulate the NOTCH1 target *c-MYC*, even if these effects do not seem to be synergistic.

#### NOTCH1 mutation has no impact on the outcome of ibrutinib-treated CLL patients in a real-life monocentric experience

The increasing number of patients under ibrutinib treatment allows the acquisition of extremely relevant real-life data at the clinical and biological levels. Here, we analyzed the efficacy of ibrutinib in a cohort of 33 patients in treatment at our institution. Baseline characteristics are shown in Supplementary Table S4. Median age was 71 years. Patients had a more advanced disease in terms of Rai or Binet stages (69% stage III–IV and 97% stage B–C, respectively). Twenty-seven percent had lymph nodes  $\geq 5$  cm. Ninety-four percent were R/R CLL with a median of two prior therapies (range, 0–6; 6% of previously untreated). Del(17p) and/or *TP53* mutation tests were performed in 29 patients and 27% were positive. *NOTCH1* mutation was present in 39% of patients analyzed with six patients harboring small subclones and significantly correlated with unmutated IGHV (77%;  $P < 0.01$ ). Cooccurrence of mutated *NOTCH1* and del(11q) or *TP53* alterations was uncommon.

The best overall response varies between *NOTCH1*-mutated versus wild-type CLL (54% vs. 68.4%, respectively) due to a lower complete remission rate and higher percentage of stable disease in mutated patients (15.5% vs. 31.6% and 46% vs. 26.3%, respectively). Median follow-up on ibrutinib was 21 months with an estimated PFS and OS of 85.5% and 78.9%, respectively (Supplementary Fig. S7). Although *NOTCH1*-mutated patients showed reduced PFS and OS compared with wild-type CLL, curve comparison did not show statistically significant differences between these groups (Supplementary Fig. S7). These data are consistent with *in vitro* evidence demonstrating that ibrutinib efficacy is independent of *NOTCH1* mutational status.

A statistical comparison of ibrutinib efficacy between patients with ICN1+ versus ICN1– CLL was not feasible, due to the extremely limited number of ICN1– samples. Indeed, the majority of patients (around 90%) displayed an active form of NOTCH1 compared with 50% described in previous analysis of Fabbri and colleagues (22). The higher incidence of ICN1+ CLL in our cohort may be related to the presence of mainly R/R CLL, suggesting a potential correlation between NOTCH1 activation and a resistant phenotype. As the median duration of response to ibrutinib in CLL prospective cohort studies inversely correlated with the number of prior therapy lines, our data further support the results of clinical trials on the use of ibrutinib as first-line therapy, when the incidence of ICN+ CLL is expected to be low.

#### NOTCH1 activity is downregulated in patients with CLL under ibrutinib treatment

We next investigated whether and how ibrutinib affected NOTCH1 activation during the course of therapy, analyzing serial purified CLL cells samples collected from patients at baseline and after different times from the initiation of therapy.

First, we examined whether the clonal frequency of the *NOTCH1*-mutated gene changed during the course of treatment. A ddPCR analysis of the *NOTCH1* mutation burden did not reveal any significant alteration from baseline during 1-year follow-up (Fig. 6A), indicating that ibrutinib has no impact on the clonal selection of *NOTCH1* mutations.

Then, we measured by Western blotting the status of the NOTCH1 activity on purified CLL cells from ibrutinib-treated patients. As shown in Fig. 6B, there was a progressive reduction of NOTCH1-ICD expression during the course of therapy. Specifically, the levels of cleaved NOTCH1 were significantly decreased starting at month 1 compared with baseline and reached approximately 5 $\times$  reduction after 1-year treatment ( $N = 18$ ;  $P < 0.01$ ). The presence of a *NOTCH1* mutation delayed the clearance of NOTCH1-ICD that was significantly reduced from baseline after 6-month treatment ( $N = 6$ ;  $P < 0.05$ ; Supplementary Fig. S8). Notably, NOTCH1 activity resulted similarly low in both *NOTCH1*-mutated and unmutated samples at 1-year follow-up.

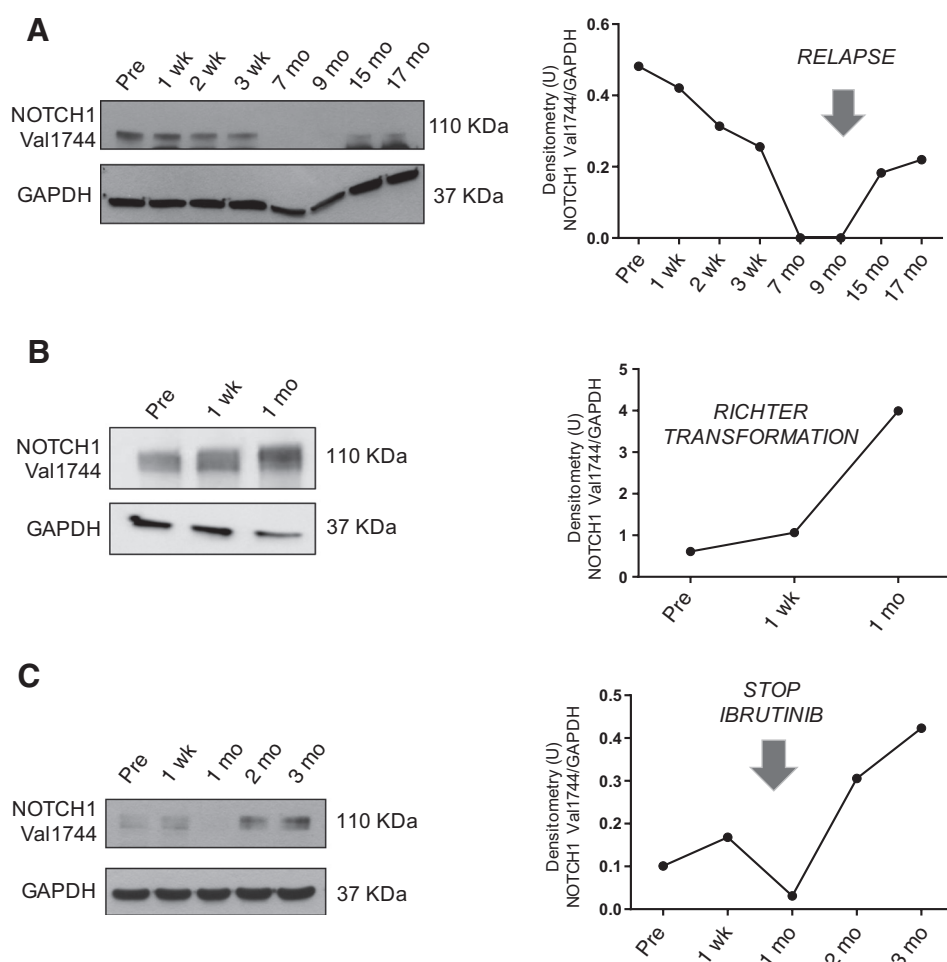
Ibrutinib treatment typically leads to the emergence of lymphocytosis that can persist for a long time even in the presence of a clinical benefit. In our patients, the reduction of NOTCH1-ICD levels by ibrutinib was more rapid and profound in patients with a lower number of lymphocytes in the PB (Fig. 6C).

Activation of NOTCH1 target genes represents a reliable read-out of NOTCH1 activity. A recent study identified *c-MYC* as a NOTCH1-transactivated gene (22). To further define the impact of ibrutinib on NOTCH1 activity, we measured mRNA expression of *c-MYC* in serial CLL samples. Our data demonstrated that this NOTCH1 target was significantly downregulated after 3 months of ibrutinib treatment ( $N = 25$ ;  $P < 0.001$ ; Fig. 6D). Conversely, a transcriptional downregulation of the *NOTCH1* gene occurred at later time points, with a significant mRNA reduction observed after 1-year treatment ( $N = 25$ ;  $P < 0.05$ ; Fig. 6D).

In keeping with *in vitro* data, these results suggest that the *in vivo* NOTCH1 activity was significantly reduced by the BTKi during treatment.

#### NOTCH1 activation is a marker of resistance, disease evolution, and treatment adherence in patients under ibrutinib therapy

Mechanisms of resistance to ibrutinib so far identified are the result of mutations in *BTK* or *PLCG2* genes. To date, these

**Figure 7.**

The levels of activated NOTCH1 protein correlated with the clinical response to ibrutinib. Kinetics of activated NOTCH1-ICD expression in the setting of ibrutinib-treated CLL at relapse (A), in a patient with Richter syndrome (B), and in a case of drug discontinuation for intolerance (C). Western blotting staining was performed using the NOTCH1(Val1744) antibody (left) and densitometry units (U) were calculated relative to GAPDH (right).

mutations precede clinical relapses in most of the cases, but the existence of other concomitant or alternative biological escape mechanisms of CLL cells treated with ibrutinib remains unclear.

**Patients 1–2.** To explore the role of NOTCH1 as a new molecular mechanism of drug resistance, we analyzed serial samples from two patients treated with ibrutinib who developed CLL progression during the course of therapy. Ibrutinib treatment of the first patient determined blood count normalization and a significant reduction of lymph node dimensions in 1 year. However, after 15-month treatment, we observed CLL progression. Sanger sequencing analysis excluded *BTK* mutations, but showed a new variant of the *PLCG2* gene (Supplementary Fig. S9). This mutation consisted in a K722R point mutation that affected the SH2 loci of the auto-inhibitory domain, the same region of the R665W mutations previously described in ibrutinib-resistant patients. We hypothesized that the newly identified K722R variant might have similar capability.

Notably, the levels of activated NOTCH1-ICD protein in cells collected during treatment directly correlated with disease activity (Fig. 7A). Upon ibrutinib treatment, NOTCH1-ICD levels decreased gradually and consistently over time and became undetectable after 7 months. Strikingly, ibrutinib-resistant CLL cells showed again a cleaved NOTCH1 band. We documented a similar clinical and NOTCH1-ICD expression trend in a second

patient lacking *BTK/PLCG2* mutations while relapsing under ibrutinib (Supplementary Fig. S10).

These data indicated that NOTCH1 deregulation was concomitant or alternative to *BTK/PLCG2* mutations in patients with CLL relapsing under ibrutinib treatment.

**Patient 3.** Despite ibrutinib's activity in CLL, treatment has to be prematurely stopped in cases of Richter transformation (RT; refs. 33, 34). We explored the role of NOTCH1 signaling in such setting, as reasons for treatment failure are still under investigation. We report a case of a patient starting ibrutinib for progressive CLL with nasopharyngeal invasion and cervical lymphadenopathy, together with del(17p). After 1 month of therapy, neck lymph node size was higher than baseline with histologic documentation of RT. The levels of activated NOTCH1-ICD in PB CD19<sup>+</sup>/CD5<sup>+</sup> cells paralleled disease transformation (Fig. 7B).

**Patient 4.** Many patients treated with ibrutinib develop adverse events, representing drug-limiting toxicity with impact on clinical outcomes. We measured NOTCH1 activity in serial samples from a patient that discontinued ibrutinib for gastrointestinal toxicity. As shown in Fig. 7C, the levels of the cleaved NOTCH1 band became barely detectable during ibrutinib treatment and increased again after drug withdrawal. These data provide further support for a link between the

antileukemic activity of ibrutinib and its capacity to modulate the NOTCH1 signaling.

## Discussion

BCR signaling plays an integral role in B-cell malignancies' development, representing a ripe target for innovative therapy in CLL. Thus, the identification of molecular mechanisms underlying BCR inhibition and novel interaction partners of the BCR has the potential to further improve CLL-targeted treatments. In this study, we provided new evidence of a relationship between the BCR pathway and NOTCH1 activity. *In vitro*, the BTK inhibitor ibrutinib impaired NOTCH1 activity while BCR stimulation increased NOTCH1-ICD levels, suggesting that BTK might be one of the regulators of NOTCH1 signaling activation in CLL.

The interaction between NOTCH and BCR has been previously described in murine primary B cells (35), in which NOTCH1 appeared as an important mediator of BCR-induced enhancement of B-cell activation. In this context, BCR stimulation increased NOTCH1 mRNA and protein expression, but not signaling activation, for which it was necessary the interaction of activated B cells with a NOTCH ligand. Conversely, our findings showed that in CLL, BCR stimulation alone was able to enhance NOTCH1 activation as evidenced by the increased nuclear levels of NOTCH1-ICD and NOTCH1 transcriptional signature. Interestingly, these data support the hypothesis of an intrinsic ligand-independent mechanism of NOTCH activation in CLL that could synergize with the BCR signaling for leukemia progression. In this respect, Thomas and colleagues (36) demonstrated that the proliferation of B cells depends on NOTCH, CD40, and BCR activity *in vitro*. Moreover, data from lymphoma cell lines suggest that NOTCH signaling might interact with BCR signaling at the level of their common downstream gene *c-MYC* to regulate cell proliferation and apoptosis (37). In agreement with the above observation, even in CLL cells, both BCR and NOTCH signaling lead to MYC activation for the leukemic clone expansion (38).

In this work, we provided new evidence for BTKi off-target effects that involve downregulation not only of NOTCH1 but also of NOTCH2 activity and JAGGED1 expression. In many tumor subtypes, ibrutinib appears to work via several intracellular signals of cancer growth demonstrating that this drug is not entirely specific in its binding to BTK (39, 40). Ibrutinib efficacy was associated to a direct anti-EGFR effect in lung cancer (41) or to the activity against EGFR-induced NF- $\kappa$ B activation in glioma (42). In addition, ibrutinib reduced phosphorylated HER2 and AKT in breast cancer (43), while sensitivity to inhibition of BTK has been demonstrated in MYC-amplified esophageal tumor lines (44). Interestingly, aberrant NOTCH signaling activation has been implicated in many of the abovementioned solid tumors (45). Therefore, our finding of the anti-NOTCH effects of ibrutinib might open new potential avenues for expanding the clinical utility of BTK inhibitors by repurposing this drug to other NOTCH-related tumors, beside CLL.

Mechanistically, the evidence that specific silencing of BTK decreased the levels of NOTCH1-ICD in CLL cells suggested that the anti-NOTCH1 effect of ibrutinib partially depends on the inhibition of BTK activity. Moreover, results of *in situ* PLA experiments showed the presence in CLL cells of NOTCH1-ICD/BTK complexes, whose number was reduced after ibrutinib treatment. On this basis, we suggest that active BTK interacts with NOTCH1-

ICD to maintain its levels, and that ibrutinib leads to NOTCH1-ICD downregulation by causing weakening of NOTCH1-ICD/BTK interactions.

We showed that when ibrutinib was used in patients with CLL, it exhibited a strong clinical activity associated with downregulation of NOTCH1 signaling. This latter effect began to be significant 1 month after the initiation of ibrutinib in patients with CLL, suggesting that pathways other than BTK, may maintain NOTCH1 signaling or contrast NOTCH1 downregulation induced by ibrutinib in early phase of treatment.

Our results showed that NOTCH1 signaling was restored at relapse and remained activated in RT. These data suggest that NOTCH1 activation contribute to counteract the antileukemic activity of ibrutinib, representing a new potential mechanism of drug resistance. In keeping with this hypothesis, we demonstrated that ibrutinib exerted *in vitro* increased cytotoxicity in CLL cells with inactive NOTCH1 compared with CLL-expressing NOTCH1-ICD. An additional clinical implication of our findings is that ibrutinib-treated patients may benefit of combinatorial drug therapy to target multiple pathways that are linked to the BCR signaling, including the NOTCH pathway. In this context, Secchiero and colleagues (46) recently described the potential antileukemic activity of the combination of ibrutinib with GSIs in primary CLL cells *in vitro*. The use of GSIs in clinical trials showed on-target toxicities that have been, in part, overcome by altering the schedule of delivery and attenuated by the use of steroids (47, 48). Thus, the identification of more selective NOTCH1 antagonists represents an alternative method to target NOTCH1 in CLL avoiding the risk of GSIs toxicity (7, 49). We recently demonstrated that bepridil is an anti-NOTCH1 molecule with antileukemic effects in preclinical models of CLL (32). Here, we demonstrated that bepridil enhanced the cytotoxic effect of ibrutinib against primary CLL cells, underlying the high potential of NOTCH-targeted therapies in overcoming CLL drug resistance. Because the effects of ibrutinib–bepridil combination do not appear to be synergistic, the individual components of BTK and NOTCH1 inhibitor combination should be carefully selected in future translational research in CLL. Moreover, to identify the patients who could benefit from these combined therapies, it would be relevant to characterize the interactions between BCR and NOTCH1 pathways in CLL subsets carrying distinct stereotyped BCR, in particular, in CLL of the stereotyped subset 8 that are characterized by a high frequency of *NOTCH1* mutations and a robust BCR signaling (50).

Our *in vitro* data showed that the cytotoxic efficacy of ibrutinib is similar in *NOTCH1*-mutated and unmutated patients. Consequently, the presence of *NOTCH1* mutations did not negatively impact the efficacy of ibrutinib on the outcome of our CLL cohort, in line with the results of prospective studies using ibrutinib in CLL. In the RESONATE trial of patients with previously treated CLL (51), the 18-month PFS with ibrutinib was similar regardless of baseline genetic *NOTCH1* status. Overall response and PFS were not influenced by the presence of *NOTCH1* mutations in a subgroup analysis of the RESONATE-17 that included only del (17p) patients (52). Evolutionary dynamics induced by targeted therapy in CLL have been analyzed by whole-exome sequencing of samples during ibrutinib therapy (53). Over the first year of treatment, BTK-targeted therapy is associated with overall clonal stability in more than half of CLLs. We described that the *NOTCH1* mutational burden in the leukemia clone did not significantly change over the first-year treatment. The general

stability of *NOTCH1*-mutated clones is consistent with prior studies reporting comparable response rates to ibrutinib for both *NOTCH*-mutated and wild-type CLL (51).

Relapse of CLL after ibrutinib is an issue of clinical significance. On the basis of published data, the cumulative incidence of discontinuation for progression is variable between patient populations ranging from 19% in the R/R (54) to 43% in high-risk CLL (5). Mutations in *BTK* and *PLC $\gamma$ 2* have emerged as main mechanisms of drug resistance (55). Specifically, the mutation of a cysteine residue of *BTK* reduced the ibrutinib-binding affinity while *PLC $\gamma$ 2* mutations promoted *BTK*-independent BCR activation (6).

However, not all patients carry these mutations (55), and there are alternative mechanisms that bypass *BTK* in other ibrutinib-resistant lymphoproliferative disorders (56). Our data point to the assessment of *NOTCH1*-ICD levels as a new marker of disease response and indicate *NOTCH1* activation as an alternative mechanism underlying acquired resistance, independent of *BTK/PLC $\gamma$ 2* mutations. It could therefore be advantageous to monitor *NOTCH1* activation status in CLL under ibrutinib treatment to track the evolution of the malignant clone for the optimization of follow-up timing and eventually inform further treatment choices.

In conclusion, we demonstrated that the therapeutic response to ibrutinib is associated with the decrease of *NOTCH1* activation, an important pathway for CLL pathogenesis. Activated *NOTCH1* represents a new mechanism of resistance and a marker to monitor disease response in CLL. All these findings not only provide further support to ibrutinib therapy optimization, but also for its exploration in combination with anti-*NOTCH1* agents in the setting of primary or acquired resistance.

### Disclosure of Potential Conflicts of Interest

No potential conflicts of interest were disclosed.

### References

- Fabbri G, Dalla-Favera R. The molecular pathogenesis of chronic lymphocytic leukaemia. *Nat Rev Cancer* 2016;16:145–62.
- Burger JA, Chiorazzi N. B cell receptor signaling in chronic lymphocytic leukemia. *Trends Immunol* 2013;34:592–601.
- Woyach JA, Johnson AJ, Byrd JC. The B-cell receptor signaling pathway as a therapeutic target in CLL. *Blood* 2012;120:1175–84.
- Herman SE, Gordon AL, Hertlein E, Ramanunni A, Zhang X, Jaglowski S, et al. Bruton tyrosine kinase represents a promising therapeutic target for treatment of chronic lymphocytic leukemia and is effectively targeted by PCI-32765. *Blood* 2011;117:6287–96.
- Byrd JC, Furman RR, Coutre SE, Flinn IW, Burger JA, Blum KA, et al. Targeting *BTK* with ibrutinib in relapsed chronic lymphocytic leukemia. *N Engl J Med* 2013;369:32–42.
- Woyach JA, Furman RR, Liu TM, Ozer HG, Zapatka M, Ruppert AS, et al. Resistance mechanisms for the Bruton's tyrosine kinase inhibitor ibrutinib. *N Engl J Med* 2014;370:2286–94.
- Rosati E, Baldoni S, De Falco F, Del Papa B, Dorillo E, Rompietti C, et al. *NOTCH1* aberrations in chronic lymphocytic leukemia. *Front Oncol* 2018; 8:229.
- Arruga F, Gizdic B, Bologna C, Cignetto S, Buonincontri R, Serra S, et al. Mutations in *NOTCH1* PEST domain orchestrate CCL19-driven homing of chronic lymphocytic leukemia cells by modulating the tumor suppressor gene *DUSP22*. *Leukemia* 2017;31:1882–93.
- Rosati E, Sabatini R, Rampino G, Tabilio A, Di Ianni M, Fettucciari K, et al. Constitutively activated Notch signaling is involved in survival and apoptosis resistance of B-CLL cells. *Blood* 2009;113: 856–65.
- Di Ianni M, Baldoni S, Rosati E, Ciurnelli R, Cavalli L, Martelli MF, et al. A new genetic lesion in B-CLL: a *NOTCH1* PEST domain mutation. *Br J Haematol* 2009;146:689–91.
- Sportoletti P, Baldoni S, Cavalli L, Del Papa B, Bonifacio E, Ciurnelli R, et al. *NOTCH1* PEST domain mutation is an adverse prognostic factor in B-CLL. *Br J Haematol* 2010;151:404–6.
- Sportoletti P, Baldoni S, Del Papa B, Cantaffa R, Ciurnelli R, Aureli P, et al. A novel *NOTCH1* PEST domain mutation in a case of chronic lymphocytic leukemia. *Leuk Lymphoma* 2013;54:1780–2.
- Fabbri G, Rasi S, Rossi D, Trifonov V, Khiabani H, Ma J, et al. Analysis of the chronic lymphocytic leukemia coding genome: role of *NOTCH1* mutational activation. *J Exp Med* 2011;208:1389–401.
- Rossi D, Rasi S, Fabbri G, Spina V, Fangazio M, Forconi F, et al. Mutations of *NOTCH1* are an independent predictor of survival in chronic lymphocytic leukemia. *Blood* 2012;119:521–9.
- Puente XS, Pinyol M, Quesada V, Conde L, Ordóñez GR, Villamor N, et al. Whole-genome sequencing identifies recurrent mutations in chronic lymphocytic leukaemia. *Nature* 2011;475:101–5.
- Wang L, Lawrence MS, Wan Y, Stojanov P, Sougnez C, Stevenson K, et al. *SF3B1* and other novel cancer genes in chronic lymphocytic leukemia. *N Engl J Med* 2011;365:2497–506.
- Landau DA, Tausch E, Taylor-Weiner AN, Stewart C, Reiter JG, Bahlo J, et al. Mutations driving CLL and their evolution in progression and relapse. *Nature* 2015;526:525–30.
- Arruga F, Gizdic B, Serra S, Vaisitti T, Ciardullo C, Coscia M, et al. Functional impact of *NOTCH1* mutations in chronic lymphocytic leukemia. *Leukemia* 2014;28:1060–70.

### Authors' Contributions

**Conception and design:** B. Del Papa, S. Baldoni, P. Sportoletti  
**Development of methodology:** B. Del Papa, S. Baldoni, E. Dorillo, F. De Falco, C. Rompietti, D. Cecchini, M.G. Cantelmi, D. Sorcini, M. Nogarotto, F.M. Adamo, F. Mezzasoma, E.C.S. Barcelos, R.I. Ostini, A.D. Tommaso, A. Marra, G. Montanaro, E. Rosati, P. Sportoletti  
**Acquisition of data (provided animals, acquired and managed patients, provided facilities, etc.):** E. Albi, R.I. Ostini, F. Falzetti, P. Sportoletti  
**Analysis and interpretation of data (e.g., statistical analysis, biostatistics, computational analysis):** B. Del Papa, S. Baldoni, E. Dorillo, F. De Falco, C. Rompietti, D. Cecchini, M.G. Cantelmi, D. Sorcini, M. Nogarotto, F.M. Adamo, F. Mezzasoma, E.C.S. Barcelos, R.I. Ostini, A.D. Tommaso, A. Marra, M.P. Martelli, F. Falzetti, M.D. Ianni, E. Rosati, P. Sportoletti  
**Writing, review, and/or revision of the manuscript:** B. Del Papa, S. Baldoni, E. Dorillo, F. De Falco, C. Rompietti, D. Cecchini, M.G. Cantelmi, D. Sorcini, M. Nogarotto, F.M. Adamo, F. Mezzasoma, E.C.S. Barcelos, E. Albi, R.I. Ostini, A.D. Tommaso, A. Marra, M.P. Martelli, F. Falzetti, M.D. Ianni, E. Rosati, P. Sportoletti  
**Administrative, technical, or material support (i.e., reporting or organizing data, constructing databases):** B. Del Papa, S. Baldoni, F. De Falco, C. Rompietti, M. Nogarotto, F.M. Adamo, E.C.S. Barcelos, E. Albi, F. Falzetti, P. Sportoletti  
**Study supervision:** P. Sportoletti

### Acknowledgments

The authors thank Tiziana Zei, Lorenzo Moretti and Giulia Formichetti for their technical support on molecular diagnostics and cellular selection. This work was supported by AIRC MFAG 2015 - ID.17442 Project - and IG 2018 - ID. 21352 Project - (principal investigator: P. Sportoletti) and from the Italian Ministry of Education, University and Research - Programma SIR N. RBS114GPBL (to P. Sportoletti), and Coordenação de Aperfeiçoamento de Pessoal de Nível Superior (CAPES) - Finance Code 19/2016 (E.C.S. Barcelos).

The costs of publication of this article were defrayed in part by the payment of page charges. This article must therefore be hereby marked *advertisement* in accordance with 18 U.S.C. Section 1734 solely to indicate this fact.

Received April 5, 2019; revised August 2, 2019; accepted September 24, 2019; published first October 2, 2019.

19. De Falco F, Sabatini R, Falzetti F, Di Ianni M, Sportoletti P, Baldoni S, et al. Constitutive phosphorylation of the active Notch1 intracellular domain in chronic lymphocytic leukemia cells with NOTCH1 mutation. *Leukemia* 2015;29:994–8.
20. Villamor N, Conde L, Martinez-Trillos A, Cazorla M, Navarro A, Bea S, et al. NOTCH1 mutations identify a genetic subgroup of chronic lymphocytic leukemia patients with high risk of transformation and poor outcome. *Leukemia* 2013;27:1100–6.
21. Puente XS, Bea S, Valdes-Mas R, Villamor N, Gutierrez-Abril J, Martin-Subero JI, et al. Non-coding recurrent mutations in chronic lymphocytic leukaemia. *Nature* 2015;526:519–24.
22. Fabbri G, Holmes AB, Viganotti M, Scuoppo C, Belver L, Herranz D, et al. Common nonmutational NOTCH1 activation in chronic lymphocytic leukemia. *Proc Natl Acad Sci U S A* 2017;114:E2911–E9.
23. Di Ianni M, Baldoni S, Del Papa B, Aureli P, Dorillo E, De Falco F, et al. NOTCH1 is aberrantly activated in chronic lymphocytic leukemia hematopoietic stem cells. *Front Oncol* 2018;8:105.
24. Yeomans A, Thirdborough SM, Valle-Argos B, Linley A, Krysov S, Hidalgo MS, et al. Engagement of the B-cell receptor of chronic lymphocytic leukemia cells drives global and MYC-specific mRNA translation. *Blood* 2016;127:449–57.
25. Sportoletti P, Baldoni S, Del Papa B, Aureli P, Dorillo E, Ruggeri L, et al. A revised NOTCH1 mutation frequency still impacts survival while the allele burden predicts early progression in chronic lymphocytic leukemia. *Leukemia* 2014;28:436–9.
26. Patnaik MM, Lasho TL, Hodnefield JM, Knudson RA, Ketterling RP, Garcia-Manero G, et al. SF3B1 mutations are prevalent in myelodysplastic syndromes with ring sideroblasts but do not hold independent prognostic value. *Blood* 2012;119:569–72.
27. Malcikova J, Tausch E, Rossi D, Sutton LA, Soussi T, Zenz T, et al. ERIC recommendations for TP53 mutation analysis in chronic lymphocytic leukemia-update on methodological approaches and results interpretation. *Leukemia* 2018;32:1070–80.
28. Ghia P, Stamatopoulos K, Belessi C, Moreno C, Stilgenbauer S, Stevenson F, et al. ERIC recommendations on IGHV gene mutational status analysis in chronic lymphocytic leukemia. *Leukemia* 2007;21:1–3.
29. De Falco F, Del Papa B, Baldoni S, Sabatini R, Falzetti F, Di Ianni M, et al. IL-4-dependent Jagged1 expression/processing is associated with survival of chronic lymphocytic leukemia cells but not with Notch activation. *Cell Death Dis* 2018;9:1160.
30. De Falco F, Sabatini R, Del Papa B, Falzetti F, Di Ianni M, Sportoletti P, et al. Notch signaling sustains the expression of Mcl-1 and the activity of eIF4E to promote cell survival in CLL. *Oncotarget* 2015;6:16559–72.
31. Pozzo F, Bittolo T, Vendramini E, Bomben R, Bulian P, Rossi FM, et al. NOTCH1-mutated chronic lymphocytic leukemia cells are characterized by a MYC-related overexpression of nucleophosmin 1 and ribosome-associated components. *Leukemia* 2017;31:2407–15.
32. Baldoni S, Del Papa B, Dorillo E, Aureli P, De Falco F, Rompietti C, et al. Bepridil exhibits anti-leukemic activity associated with NOTCH1 pathway inhibition in chronic lymphocytic leukemia. *Int J Cancer* 2018;143:958–70.
33. Jain P, Keating M, Wierda W, Estrov Z, Ferrajoli A, Jain N, et al. Outcomes of patients with chronic lymphocytic leukemia after discontinuing ibrutinib. *Blood* 2015;125:2062–7.
34. Albi E, Baldoni S, Aureli P, Dorillo E, Del Papa B, Ascani S, et al. Ibrutinib treatment of a patient with relapsing chronic lymphocytic leukemia and sustained remission of Richter syndrome. *Tumori* 2017;103:e37–e40.
35. Kang JA, Kim WS, Park SG. Notch1 is an important mediator for enhancing of B-cell activation and antibody secretion by Notch ligand. *Immunology* 2014;143:550–9.
36. Thomas M, Calamito M, Srivastava B, Maillard I, Pear WS, Allman D. Notch activity synergizes with B-cell-receptor and CD40 signaling to enhance B-cell activation. *Blood* 2007;109:3342–50.
37. He F, Wang L, Hu XB, Yin DD, Zhang P, Li GH, et al. Notch and BCR signaling synergistically promote the proliferation of Raji B-lymphoma cells. *Leuk Res* 2009;33:798–802.
38. Rossi D. MYC addiction in chronic lymphocytic leukemia. *Leuk Lymphoma* 2013;54:905–6.
39. Berglof A, Hamasy A, Meinke S, Palma M, Krstic A, Mansson R, et al. Targets for ibrutinib beyond B cell malignancies. *Scand J Immunol* 2015;82:208–17.
40. Tissino E, Benedetti D, Herman SEM, Ten Hacken E, Ahn IE, Chaffee KG, et al. Functional and clinical relevance of VLA-4 (CD49d/CD29) in ibrutinib-treated chronic lymphocytic leukemia. *J Exp Med* 2018;215:681–97.
41. Gao W, Wang M, Wang L, Lu H, Wu S, Dai B, et al. Selective antitumor activity of ibrutinib in EGFR-mutant non-small cell lung cancer cells. *J Natl Cancer Inst* 2014;106:dju204.
42. Yue C, Niu M, Shan QQ, Zhou T, Tu Y, Xie P, et al. High expression of Bruton's tyrosine kinase (BTK) is required for EGFR-induced NF-kappaB activation and predicts poor prognosis in human glioma. *J Exp Clin Cancer Res* 2017;36:132.
43. Wang X, Wong J, Sevinsky CJ, Kokabee L, Khan F, Sun Y, et al. Bruton's tyrosine kinase inhibitors prevent therapeutic escape in breast cancer cells. *Mol Cancer Ther* 2016;15:2198–208.
44. Chong IY, Aronson L, Bryant H, Gulati A, Campbell J, Elliott R, et al. Mapping genetic vulnerabilities reveals BTK as a novel therapeutic target in oesophageal cancer. *Gut* 2018;67:1780–92.
45. Huang T, Zhou Y, Cheng AS, Yu J, To KF, Kang W. NOTCH receptors in gastric and other gastrointestinal cancers: oncogenes or tumor suppressors? *Mol Cancer* 2016;15:80.
46. Secchiero P, Voltan R, Rimondi E, Melloni E, Athanasakis E, Tisato V, et al. The  $\gamma$ -secretase inhibitors enhance the anti-leukemic activity of ibrutinib in B-CLL cells. *Oncotarget* 2017;8:59235–45.
47. Krop I, Demuth T, Guthrie T, Wen PY, Mason WP, Chinnaiyan P, et al. Phase I pharmacologic and pharmacodynamic study of the gamma secretase (Notch) inhibitor MK-0752 in adult patients with advanced solid tumors. *J Clin Oncol* 2012;30:2307–13.
48. Real PJ, Tosello V, Palomero T, Castillo M, Hernando E, de Stanchina E, et al. Gamma-secretase inhibitors reverse glucocorticoid resistance in T cell acute lymphoblastic leukemia. *Nat Med* 2009;15:50–8.
49. Lopez-Guerra M, Xargay-Torrent S, Rosich L, Montraveta A, Roldan J, Matas-Cespedes A, et al. The  $\gamma$ -secretase inhibitor PF-03084014 combined with fludarabine antagonizes migration, invasion and angiogenesis in NOTCH1-mutated CLL cells. *Leukemia* 2015;29:96–106.
50. Rossi D, Spina V, Bomben R, Rasi S, Dal-Bo M, Brusca A, et al. Association between molecular lesions and specific B-cell receptor subsets in chronic lymphocytic leukemia. *Blood* 2013;121:4902–5.
51. Brown JR, Hillmen P, O'Brien S, Barrientos JC, Reddy NM, Coutre SE, et al. Extended follow-up and impact of high-risk prognostic factors from the phase 3 RESONATE study in patients with previously treated CLL/SLL. *Leukemia* 2018;32:83–91.
52. Boddu P, Ferrajoli A. Prognostic factors in the era of targeted therapies in CLL. *Curr Hematol Malig Rep* 2018;13:78–90.
53. Landau DA, Sun C, Rosebrock D, Herman SEM, Fein J, Sivina M, et al. The evolutionary landscape of chronic lymphocytic leukemia treated with ibrutinib targeted therapy. *Nat Commun* 2017;8:2185.
54. Woyach JA, Ruppert AS, Guinn D, Lehman A, Blachly JS, Lozanski A, et al. BTK(C481S)-mediated resistance to ibrutinib in chronic lymphocytic leukemia. *J Clin Oncol* 2017;35:1437–43.
55. Lampson BL, Brown JR. Are BTK and PLCG2 mutations necessary and sufficient for ibrutinib resistance in chronic lymphocytic leukemia? *Expert Rev Hematol* 2018;11:185–94.
56. Zhang SQ, Smith SM, Zhang SY, Lynn Wang Y. Mechanisms of ibrutinib resistance in chronic lymphocytic leukaemia and non-Hodgkin lymphoma. *Br J Haematol* 2015;170:445–56.